

The High Energy Limit of QCD: BFKL Cross Sections*

AGUSTÍN SABIO VERA

Physics Department, Theory Division, CERN, CH-1211 Geneva 23, Switzerland

In this contribution we describe in some detail different aspects of the construction of BFKL cross sections. We focus on several effects which are relevant at next-to-leading order. In particular, we describe QCD coherence in DIS final states, improvements of the collinear region in multi-Regge kinematics, inclusive jet production at next-to-leading order, and azimuthal angle decorrelations of Mueller-Navelet jets at hadron colliders.

1. Introduction

When dealing with the description of scattering amplitudes at very high center-of-mass energies a very useful formalism is the Balitsky-Fadin-Kuraev-Lipatov (BFKL) approach [1, 2, 3, 4, 5]. In the Regge limit the dominant degrees of freedom are t -channel “Reggeized” gluons which interact with each other via standard gluons in the s -channel and a gauge invariant Reggeized gluon - Reggeized gluon - gluon vertex. This picture emerges as a consequence of multi-Regge kinematics where gluon evolution takes place with ordering in longitudinal components but not in transverse momenta. At very high energies this structure should be modified to include unitarization corrections. However, there should be a window at present and future colliders where the BFKL predictions provide a good description of the experimental data.

When terms of the form $(\alpha_s \ln s)^n$ are resummed we are in the leading-logarithmic approximation (LLA). In this limit the strong coupling does not run and α_s is a constant parameter. We should have written $\ln s/s_0$ but it turns out that in the LLA we are free to choose any s_0 . This means that there is a lot of freedom in the LLA when trying to fit experimental data. This theory is much more constrained when we include terms of the form $\alpha_s(\alpha_s \ln s)^n$. In this next-to-leading logarithmic approximation (NLLA) the coupling is allowed to run and the energy scale s_0 has to be determined.

* Presented at School on QCD, Low x Physics, Saturation and Diffraction, Copanello (Calabria, Italy), July 1-14 2007

As a matter of fact, cross sections are constructed to be independent of s_0 at NLO. However, different choices of this scale do affect higher orders in the resummation which might be important when making BFKL predictions.

In the coming sections we discuss several important aspects to take into account when constructing BFKL cross sections beyond the LLA. In section 2 we describe final states at small Bjorken x in Deep Inelastic Scattering (DIS). The idea of colour coherence is introduced and its implementation in the CCFM equation discussed. The predictions for jet rates are the same at LO when the CCFM or BFKL equations are used and we explain why. In section 3 it is shown that the region of applicability of multi-Regge kinematics can be extended to also include regions with collinear emissions. In this case there exists an interesting structure at higher orders which can be cast into a Bessel function of the first kind accounting for double logarithms in transverse scales. Up to the NLLA this double logarithms also appear in the inclusive production of a jet centrality emitted in rapidity at a hadron collider. In this case impact factors and the emission vertex of the central jet have to be modified. This is explained in some detail in section 4. Finally, in section 5 we show how the $SL(2, C)$ invariance present in the BFKL hamiltonian for non-zero momentum transfer appears in the azimuthal angle dependence of multijet events. As an example we discuss the case with two hard external scales of Mueller-Navelet jets at a hadron collider.

2. DIS final states at small x and the CCFM equation

In QED coherence suppresses soft bremsstrahlung from electron-positron pairs. In QCD processes such as $g \rightarrow q\bar{q}$ soft gluons at an angle from one of the fermionic lines larger than the angle of emission in the $q\bar{q}$ pair resolve the total colour charge of the pair. This is the same as that of the parent gluon and radiation occurs as if the soft gluon was emitted from it. This “colour coherence” can be put as angular ordered sequential gluon emissions.

If the $(i - 1)$ th emitted gluon from the proton in DIS has energy E_{i-1} , then a gluon radiated from it with a fraction $(1 - z_i)$ of its energy and a transverse momentum q_i has opening angle

$$\theta_i \approx \frac{q_i}{(1 - z_i)E_{i-1}}, \quad z_i = \frac{E_i}{E_{i-1}}. \quad (1)$$

Colour coherence leads to angular ordering with increasing opening angles towards the hard scale (the photon). We then have $\theta_{i+1} > \theta_i$, or

$$\frac{q_{i+1}}{1 - z_{i+1}} > \frac{z_i q_i}{1 - z_i}, \quad (2)$$

which reduces to $q_{i+1} > z_i q_i$ in the limit $z_i, z_{i+1} \ll 1$. In [6, 7, 8, 9] the BFKL equation for the unintegrated structure function was obtained in a

form suitable for the study of exclusive observables:

$$f_\omega(\mathbf{k}) = f_\omega^0(\mathbf{k}) + \bar{\alpha}_S \int \frac{d^2\mathbf{q}}{\pi q^2} \int_0^1 \frac{dz}{z} z^\omega \Delta_R(z, k) \Theta(q - \mu) f_\omega(\mathbf{q} + \mathbf{k}). \quad (3)$$

μ is a collinear cutoff, \mathbf{q} the transverse momentum of the emission, and

$$\Delta_R(z_i, k_i) = \exp \left[-\bar{\alpha}_S \ln \frac{1}{z_i} \ln \frac{k_i^2}{\mu^2} \right], \quad (4)$$

with $k_i \equiv |\mathbf{k}_i|$, and $\bar{\alpha}_S \equiv \alpha_S N_c / \pi$. This expression predicts gluon emissions with the virtual corrections summed to all orders. Since f_ω is an inclusive structure function, it includes the sum over final states. After this sum the μ -dependence cancels.

To get the structure function we integrate over $\mu^2 \leq q_i^2 \leq Q^2$:

$$F_{0\omega}(Q, \mu) \equiv \Theta(Q - \mu) + \sum_{r=1}^{\infty} \int_{\mu^2}^{Q^2} \prod_{i=1}^r \frac{d^2\mathbf{q}_i}{\pi q_i^2} dz_i \frac{\bar{\alpha}_S}{z_i} z_i^\omega \Delta_R(z_i, k_i), \quad (5)$$

with i being each gluon emission. A fixed number r of emitted gluons gives

$$F_{0\omega}(Q) = \int_0^1 dx x^\omega F_0(x, Q) = 1 + \sum_{r=1}^{\infty} F_{0\omega}^{(r)}(Q). \quad (6)$$

The expansion for $F_{0\omega}^{(r)}(Q, \mu)$ reads [7]

$$F_{0\omega}^{(r)}(Q, \mu) = \sum_{n=r}^{\infty} C_0^{(r)}(n; T) \frac{\bar{\alpha}_S^n}{\omega^n}, \quad (7)$$

with $T \equiv \ln(Q/\mu)$. Therefore:

$$F_{0\omega}(Q) \equiv \sum_{i=0}^{\infty} F_{0\omega}^{(i)}(Q) = \left(\frac{Q^2}{\mu^2} \right)^{\bar{\gamma}}, \quad (8)$$

where $\bar{\gamma}$ is the BFKL anomalous dimension.

Including coherence in the BFKL expressions, we get [6, 7, 8, 9]:

$$F_\omega(Q, \mu) = \Theta(Q - \mu) + \sum_{r=1}^{\infty} \int_0^{Q^2} \prod_{i=1}^r \frac{d^2\mathbf{q}_i}{\pi q_i^2} dz_i \frac{\bar{\alpha}_S}{z_i} z_i^\omega \Delta(z_i, q_i, k_i) \Theta(q_i - z_{i-1} q_{i-1}), \quad (9)$$

where $\Delta_R(z_i, k_i)$ is now the CCFM one

$$\Delta(z_i, q_i, k_i) = \exp \left[-\bar{\alpha}_S \ln \frac{1}{z_i} \ln \frac{k_i^2}{z_i q_i^2} \right]; \quad k_i > q_i. \quad (10)$$

For the first emission $q_0 z_0 = \mu$. The expansion of $F_\omega^{(r)}(Q)$ is

$$F_\omega^{(r)}(Q) = \sum_{n=r}^{\infty} \sum_{m=1}^n C^{(r)}(n, m; T) \frac{\bar{\alpha}_S^n}{\omega^{2n-m}}. \quad (11)$$

The collinear cutoff is only needed in the first emission since subsequent emissions are regulated by angular ordering.

The rates of emission of a number of gluons with transverse momentum larger than a scale μ_R , with $\mu \ll \mu_R \ll Q$, plus any number of unresolved ones, were calculated in [10] in the LLA to $\bar{\alpha}_S^3$. It was found that the jet rates both in the BFKL and CCFM approaches are the same:

$$0 \text{ jet} = \frac{(2\bar{\alpha}_S)}{\omega} S + \frac{(2\bar{\alpha}_S)^2}{\omega^2} \left[\frac{S^2}{2} \right] + \frac{(2\bar{\alpha}_S)^3}{\omega^3} \left[\frac{S^3}{6} \right], \quad (12)$$

$$\begin{aligned} 1 \text{ jet} &= \frac{(2\bar{\alpha}_S)}{\omega} T + \frac{(2\bar{\alpha}_S)^2}{\omega^2} \left[TS - \frac{1}{2} T^2 \right] \\ &+ \frac{(2\bar{\alpha}_S)^3}{\omega^3} \left[\frac{1}{3} T^3 - \frac{1}{2} T^2 S + \frac{1}{2} T S^2 \right], \end{aligned} \quad (13)$$

$$2 \text{ jet} = \frac{(2\bar{\alpha}_S)^2}{\omega^2} [T^2] + \frac{(2\bar{\alpha}_S)^3}{\omega^3} \left[T^2 S - \frac{7}{6} T^3 \right], \quad (14)$$

$$3 \text{ jet} = \frac{(2\bar{\alpha}_S)^3}{\omega^3} [T^3], \quad (15)$$

with $T = \ln(Q/\mu_R)$ and $S = \ln(\mu_R/\mu)$. This holds also to all orders in the coupling [11] since a generating function for the jet multiplicity distribution was obtained in [12]:

$$R_\omega^{(n \text{ jet})}(Q, \mu_R) = \frac{F_\omega^{(n \text{ jet})}(Q, \mu_R, \mu)}{F_\omega(Q, \mu)} = \frac{1}{n!} \frac{\partial^n}{\partial u^n} R_\omega(u, T) \Big|_{u=0}, \quad (16)$$

where the jet-rate generating function R_ω is given by

$$R_\omega(u, T) = \exp\left(-\frac{2\bar{\alpha}_s}{\omega} T\right) \left[1 + (1-u) \frac{2\bar{\alpha}_s}{\omega} T \right]^{\frac{u}{1-u}}, \quad (17)$$

with the same generating function when coherence is included. The mean number of jets and the mean square fluctuation are

$$\langle n \rangle = \frac{\partial}{\partial u} R_\omega(u, T) \Big|_{u=1} = \frac{2\bar{\alpha}_s}{\omega} T + \frac{1}{2} \left(\frac{2\bar{\alpha}_s}{\omega} T \right)^2, \quad (18)$$

$$\langle n^2 \rangle - \langle n \rangle^2 = \frac{2\bar{\alpha}_s}{\omega} T + \frac{3}{2} \left(\frac{2\bar{\alpha}_s}{\omega} T \right)^2 + \frac{2}{3} \left(\frac{2\bar{\alpha}_s}{\omega} T \right)^3. \quad (19)$$

In [13, 14] all subleading logarithms of Q^2/μ_R^2 were included and the jet multiplicity in Higgs production at the LHC was found. It has also been shown that for any sufficiently inclusive observables the CCFM formalism leads to the same results as the BFKL equation [15]. The implementation of CCFM in Monte Carlo event generators is discussed in, *e.g.*, [16, 17, 18, 19]. A numerical method suitable to investigate BFKL and CCFM in the NLLA in DIS is described in Ref. [20, 21, 22, 23].

3. Beyond multi-Regge kinematics in the collinear region

In [24] multi-Regge kinematics was extended to include collinear contributions to all orders in the BFKL framework. In [25] it was proved that this collinear region hides a very interesting structure in terms of double logarithms. A renormalization group (RG)-improved kernel was obtained which does not mix transverse with longitudinal momentum components.

In $\overline{\text{MS}}$ renormalisation the BFKL kernel in NLA reads [26, 27]

$$\begin{aligned} \int d^2\vec{q}_2 \mathcal{K}(\vec{q}_1, \vec{q}_2) f(q_2^2) = \\ \int \frac{d^2\vec{q}_2}{|q_1^2 - q_2^2|} \left\{ \left[\bar{\alpha}_s + \bar{\alpha}_s^2 \left(\mathcal{S} - \frac{\beta_0}{4N_c} \ln \left(\frac{|q_1^2 - q_2^2|^2}{\max(q_1^2, q_2^2) \mu^2} \right) \right) \right] \right. \\ \times \left(f(q_2^2) - 2 \frac{\min(q_1^2, q_2^2)}{(q_1^2 + q_2^2)} f(q_1^2) \right) \\ \left. \times - \frac{\bar{\alpha}_s^2}{4} \left(\mathcal{T}(q_1^2, q_2^2) + \ln^2 \left(\frac{q_1^2}{q_2^2} \right) \right) f(q_2^2) \right\}, \quad (20) \end{aligned}$$

with $\beta_0 = (11N_c - 2n_f)/3$, $\mathcal{S} = (4 - \pi^2 + 5\beta_0/N_c)/12$. $\mathcal{T}(q_1^2, q_2^2)$ can be found in [26]. The action on the eigenfunctions at LLA is

$$\int d^2\vec{q}_2 \mathcal{K}(\vec{q}_1, \vec{q}_2) \left(\frac{\bar{\alpha}_s(q_2^2)}{\bar{\alpha}_s(q_1^2)} \right)^{-\frac{1}{2}} \left(\frac{q_2^2}{q_1^2} \right)^{\gamma-1} = \bar{\alpha}_s(q_1^2) \chi_0(\gamma) + \bar{\alpha}_s^2 \chi_1(\gamma). \quad (21)$$

We have used

$$\chi_0(\gamma) = 2\psi(1) - \psi(\gamma) - \psi(1 - \gamma), \quad (22)$$

$$\begin{aligned} \chi_1(\gamma) = \mathcal{S}\chi_0(\gamma) + \frac{1}{4}(\psi''(\gamma) + \psi''(1 - \gamma)) - \frac{1}{4}(\phi(\gamma) + \phi(1 - \gamma)) + \frac{3}{2}\zeta_3 \\ - \frac{\pi^2 \cos(\pi\gamma)}{4 \sin^2(\pi\gamma)(1 - 2\gamma)} \left(3 + \left(1 + \frac{n_f}{N_c^3} \right) \frac{(2 + 3\gamma(1 - \gamma))}{(3 - 2\gamma)(1 + 2\gamma)} \right) - \frac{\beta_0}{8N_c} \chi_0^2(\gamma). \quad (23) \end{aligned}$$

$\psi(\gamma) = \Gamma'(\gamma)/\Gamma(\gamma)$ and

$$\begin{aligned} \phi(\gamma) + \phi(1-\gamma) = \\ \sum_{m=0}^{\infty} \left(\frac{1}{\gamma+m} + \frac{1}{1-\gamma+m} \right) \left(\psi' \left(\frac{2+m}{2} \right) - \psi' \left(\frac{1+m}{2} \right) \right). \end{aligned} \quad (24)$$

The poles in the collinear regions $\gamma = 0, 1$ are

$$\chi_0(\gamma) \simeq \frac{1}{\gamma} + \{\gamma \rightarrow 1-\gamma\}, \quad (25)$$

$$\chi_1(\gamma) \simeq \frac{a}{\gamma} + \frac{b}{\gamma^2} - \frac{1}{2\gamma^3} + \{\gamma \rightarrow 1-\gamma\}. \quad (26)$$

where

$$a = \frac{5}{12} \frac{\beta_0}{N_c} - \frac{13}{36} \frac{n_f}{N_c^3} - \frac{55}{36}, \quad b = -\frac{1}{8} \frac{\beta_0}{N_c} - \frac{n_f}{6N_c^3} - \frac{11}{12}. \quad (27)$$

The cubic poles compensate for similar terms appearing when $s_0 = q_1 q_2$ is shifted to the DIS choice $s_0 = q_{1,2}^2$. Higher order terms beyond the NLLA, not compatible with RG evolution, are also generated by this change of scale. The truncation of the perturbative expansion is the reason why the gluon Green's function develops unphysical oscillations in the q_1^2/q_2^2 ratio.

To remove the most important terms in γ -space incompatible with RG evolution we simply perform the shift [24]:

$$\begin{aligned} \omega = & \bar{\alpha}_s \left(1 + \left(a + \frac{\pi^2}{6} \right) \bar{\alpha}_s \right) \\ & \times \left(2\psi(1) - \psi \left(\gamma + \frac{\omega}{2} - b \bar{\alpha}_s \right) - \psi \left(1 - \gamma + \frac{\omega}{2} - b \bar{\alpha}_s \right) \right) \\ & + \bar{\alpha}_s^2 \left(\chi_1(\gamma) + \left(\frac{1}{2} \chi_0(\gamma) - b \right) (\psi'(\gamma) + \psi'(1-\gamma)) - \left(a + \frac{\pi^2}{6} \right) \chi_0(\gamma) \right). \end{aligned} \quad (28)$$

To solve this equation we consider the ω -shift in the form

$$\begin{aligned} \frac{\omega}{\bar{\alpha}_s (1 + A \bar{\alpha}_s)} = & 2\psi(1) - \psi \left(\gamma + \frac{\omega}{2} + B \bar{\alpha}_s \right) - \psi \left(1 - \gamma + \frac{\omega}{2} + B \bar{\alpha}_s \right) \\ = & \sum_{m=0}^{\infty} \left(\frac{1}{\gamma + m + \frac{\omega}{2} + B \bar{\alpha}_s} + \frac{1}{1 - \gamma + m + \frac{\omega}{2} + B \bar{\alpha}_s} - \frac{2}{m+1} \right). \end{aligned} \quad (29)$$

We can now add all the approximated solutions at the different poles plus a subtraction term to enforce convergence:

$$\omega = \sum_{m=0}^{\infty} \left\{ -(1 + 2m + 2B \bar{\alpha}_s) + |\gamma + m + B \bar{\alpha}_s| \left(1 + \frac{2\bar{\alpha}_s (1 + A \bar{\alpha}_s)}{(\gamma + m + B \bar{\alpha}_s)^2} \right)^{\frac{1}{2}} \right\}$$

$$+ |1 - \gamma + m + B\bar{\alpha}_s| \left(1 + \frac{2\bar{\alpha}_s(1 + A\bar{\alpha}_s)}{(1 - \gamma + m + B\bar{\alpha}_s)^2} \right)^{\frac{1}{2}} - \frac{2\bar{\alpha}_s(1 + A\bar{\alpha}_s)}{m + 1} \Big\}. \quad (30)$$

To match the original kernel at NLLA we set $A = a$ and $B = -b$. The full NLLA scale invariant kernel without double counting terms then reads:

$$\begin{aligned} \omega &= \bar{\alpha}_s \chi_0(\gamma) + \bar{\alpha}_s^2 \chi_1(\gamma) \quad (31) \\ &+ \left\{ \sum_{m=0}^{\infty} \left[\left(\sum_{n=0}^{\infty} \frac{(-1)^n (2n)!}{2^n n! (n+1)!} \frac{(\bar{\alpha}_s + a\bar{\alpha}_s^2)^{n+1}}{(\gamma + m - b\bar{\alpha}_s)^{2n+1}} \right) \right. \right. \\ &\quad \left. \left. - \frac{\bar{\alpha}_s}{\gamma + m} - \bar{\alpha}_s^2 \left(\frac{a}{\gamma + m} + \frac{b}{(\gamma + m)^2} - \frac{1}{2(\gamma + m)^3} \right) \right] + \{\gamma \rightarrow 1 - \gamma\} \right\}. \end{aligned}$$

This result reproduces the ω -shift very closely, see Fig. 1. It is very important to note that in Eq. (31) the ω -space is decoupled from the γ -representation. In [25] an expression for the collinearly improved BFKL kernel which does not mix longitudinal with transverse degrees of freedom was obtained. To introduce the new kernel we only need to remove the term

$$- \frac{\bar{\alpha}_s^2}{4} \frac{1}{(\vec{q} - \vec{k})^2} \ln^2 \left(\frac{q^2}{k^2} \right) \quad (32)$$

in the emission part of the original kernel in the NLLA and replace it with

$$\begin{aligned} \frac{1}{(\vec{q} - \vec{k})^2} \left\{ \left(\frac{q^2}{k^2} \right)^{-b\bar{\alpha}_s \frac{|k-q|}{k-q}} \sqrt{\frac{2(\bar{\alpha}_s + a\bar{\alpha}_s^2)}{\ln^2 \left(\frac{q^2}{k^2} \right)}} J_1 \left(\sqrt{2(\bar{\alpha}_s + a\bar{\alpha}_s^2) \ln^2 \left(\frac{q^2}{k^2} \right)} \right) \right. \\ \left. - \bar{\alpha}_s - a\bar{\alpha}_s^2 + b\bar{\alpha}_s^2 \frac{|k-q|}{k-q} \ln \left(\frac{q^2}{k^2} \right) \right\}. \quad (33) \end{aligned}$$

For small differences between the q^2 and k^2 scales then

$$J_1 \left(\sqrt{2\bar{\alpha}_s \ln^2 \left(\frac{q^2}{k^2} \right)} \right) \simeq \sqrt{\frac{\bar{\alpha}_s}{2} \ln^2 \left(\frac{q^2}{k^2} \right)}, \quad (34)$$

and it does not change the ‘‘Regge-like’’ region. When the ratio of transverse momenta is large then

$$J_1 \simeq \left(\frac{2}{\pi^2 \bar{\alpha}_s \ln^2 \left(\frac{q^2}{k^2} \right)} \right)^{\frac{1}{4}} \cos \left(\sqrt{2\bar{\alpha}_s \ln^2 \left(\frac{q^2}{k^2} \right)} - \frac{3\pi}{4} \right), \quad (35)$$

removing the unphysical oscillations. This new kernel has been successfully applied to extend the region of applicability of NLLA BFKL calculations in the case of electroproduction of light vector mesons in [28].

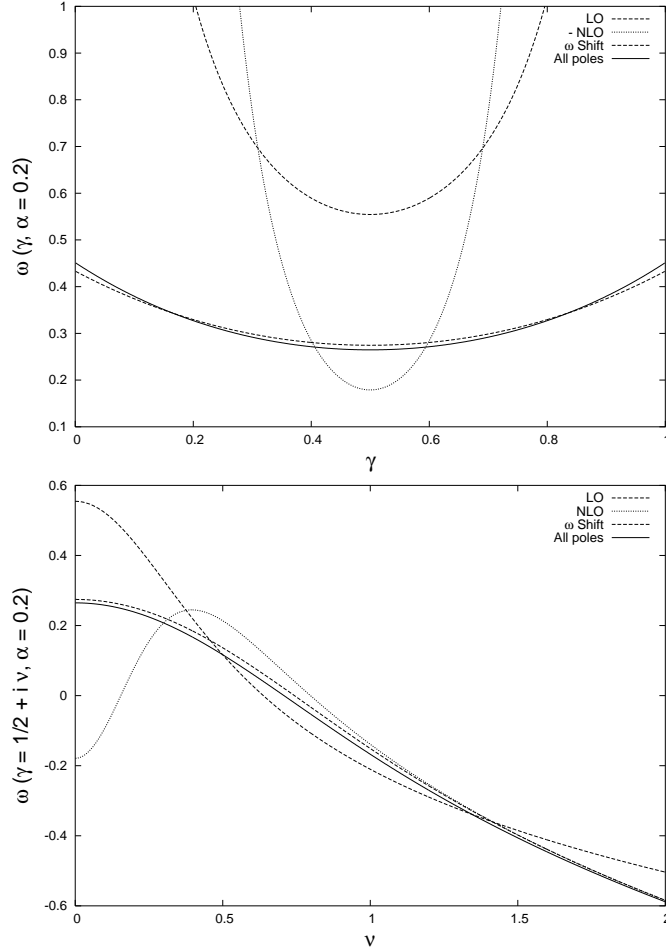


Fig. 1. The RG-improved kernel compared to its “all-poles” approximation together with the LO and NLO BFKL kernels.

4. Inclusive jet production at NLO

Now we discuss the natural choice of s_0 when a hard jet is produced in the central region of rapidity [29]. Let us start with the symmetric case of $\gamma^*\gamma^*$ scattering with the virtualities of the two photons being large and of the same order. Here the rapidities of the emitted particles are the natural variables to characterize multijet production since all transverse momenta are of the same order. The rapidity difference between two emissions is

$$y_i - y_{i+1} = \ln \frac{s_{i,i+1}}{\sqrt{\mathbf{k}_i^2 \mathbf{k}_{i+1}^2}} \quad (36)$$

which supports the choice $s_{R;i,i+1} = \sqrt{\mathbf{k}_i^2 \mathbf{k}_{i+1}^2}$ for the internal energy scales shown in Fig. 2. In hadronic collisions MRK has to be modified to include

$$\text{MRK: } p_A^2 \sim p_B^2 \sim \mathbf{k}_i^2 \sim \mathbf{k}_j^2 \gg \Lambda_{\text{QCD}}^2, \quad y_A = y_0 \gg y_1 \gg \dots \gg y_n \gg y_{n+1} = y_B$$

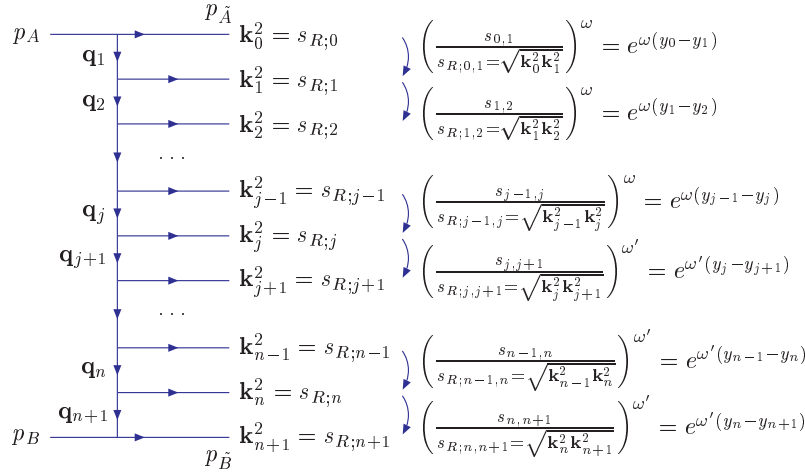


Fig. 2. $2 \rightarrow 2 + (n-1) + \text{jet}$ amplitude in the symmetric configuration with MRK. The produced jet has rapidity $y_J = y_j$ and transverse momentum $\mathbf{k}_J = \mathbf{k}_j$.

evolution in the transverse momenta, since the momentum of the jet is larger than the typical transverse scale associated to the hadron. This can be done by changing the description of the evolution from one in terms of rapidities to another in terms of longitudinal momentum fractions of the Reggeized gluons. Whereas in LO this change of scales has no consequences, in NLO accuracy it leads to modifications, not only of the jet emission vertex but also of the evolution kernels above and below the jet vertex.

In more detail, we write the solution to the BFKL equation iteratively:

$$\int d^2 \mathbf{k}_a f_\omega(\mathbf{k}_a, \mathbf{q}_a) = \frac{1}{\omega} \sum_{j=1}^{\infty} \left[\prod_{i=1}^{j-1} \int d^2 \mathbf{q}_i \frac{1}{\omega} \mathcal{K}(\mathbf{q}_i, \mathbf{q}_{i+1}) \right], \quad (37)$$

where $\mathbf{q}_1 = \mathbf{k}_a$ and $\mathbf{q}_j = \mathbf{q}_a$, and think of one side of the evolution towards the hard scale using Fig. 3 as a guide. In the symmetric case the cross section contains the following evolution between particle A and the jet:

$$\begin{aligned} \frac{d\sigma}{d^2 \mathbf{k}_J dy_J} &= \int d^2 \mathbf{q}_a \int d^2 \mathbf{k}_a \frac{\Phi_A(\mathbf{k}_a)}{2\pi \mathbf{k}_a^2} \\ &\times \int \frac{d\omega}{2\pi i} f_\omega(\mathbf{k}_a, \mathbf{q}_a) \left(\frac{s_{AJ}}{\sqrt{\mathbf{k}_a^2 \mathbf{k}_J^2}} \right)^\omega \mathcal{V}(\mathbf{q}_a, \mathbf{q}_b; \mathbf{k}_J, y_J) \dots \quad (38) \end{aligned}$$

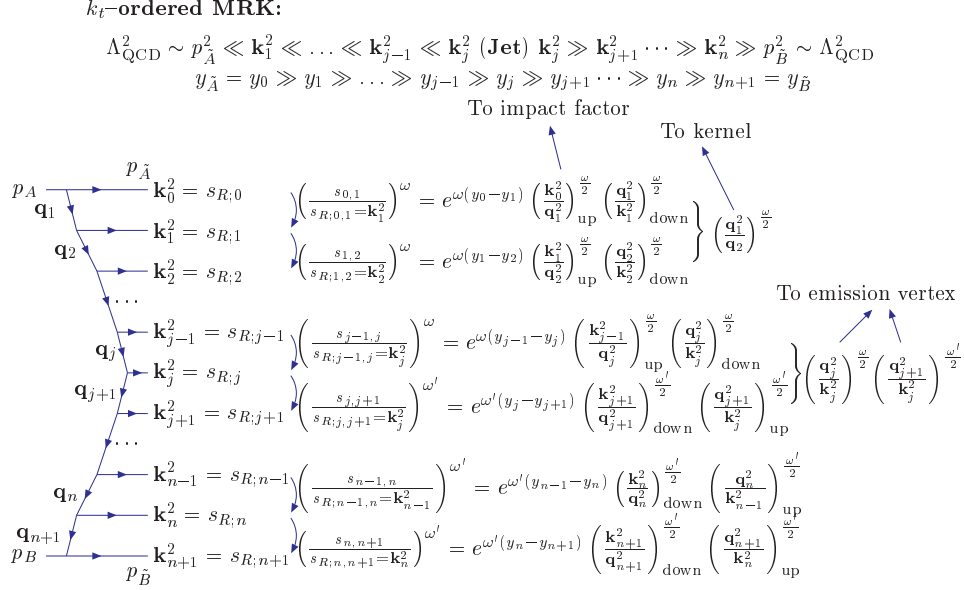


Fig. 3. $2 \rightarrow 2 + (n - 1) + \text{jet}$ amplitude in the asymmetric configuration with k_t -ordered MRK.

In the asymmetric situation where $\mathbf{k}_j^2 \gg \mathbf{k}_a^2$ the scale $\sqrt{\mathbf{k}_a^2 \mathbf{k}_j^2}$ should be replaced by \mathbf{k}_j^2 . We then rewrite the term related to the choice of energy scale. Following Fig. 3 we take $\mathbf{k}_j = \mathbf{k}_J$, $\mathbf{k}_0 = -\mathbf{k}_a = -\mathbf{q}_1$ and $\mathbf{q}_j = \mathbf{q}_a$. It is convenient to introduce a chain of scale changes in every kernel:

$$\left(\frac{s_{AJ}}{\sqrt{\mathbf{k}_a^2 \mathbf{k}_j^2}} \right)^\omega = \left[\prod_{i=1}^j \left(\frac{\mathbf{k}_i^2}{\mathbf{k}_{i-1}^2} \right)^{\frac{\omega}{2}} \right] \left(\frac{s_{AJ}}{\mathbf{k}_J^2} \right)^\omega, \quad (39)$$

which can also be written in terms of the t -channel momenta as

$$\left(\frac{s_{AJ}}{\sqrt{\mathbf{k}_a^2 \mathbf{k}_j^2}} \right)^\omega = \left[\prod_{i=1}^{j-1} \left(\frac{\mathbf{q}_{i+1}^2}{\mathbf{q}_i^2} \right)^{\frac{\omega}{2}} \right] \left(\frac{\mathbf{k}_J^2}{\mathbf{q}_a^2} \right)^{\frac{\omega}{2}} \left(\frac{s_{AJ}}{\mathbf{k}_J^2} \right)^\omega. \quad (40)$$

In this way we are changing the evolution from a difference in rapidity:

$$\frac{s_{AJ}}{\sqrt{\mathbf{k}_a^2 \mathbf{k}_j^2}} = e^{y_{\bar{A}} - y_J} \quad (41)$$

to the inverse of the longitudinal momentum fraction, *i.e.*

$$\frac{s_{AJ}}{\mathbf{k}_J^2} = \frac{1}{\alpha_J}. \quad (42)$$

This shift in scales affects the expression for the cross section:

$$\begin{aligned} \frac{d\sigma}{d^2\mathbf{k}_J dy_J} &= \int \frac{d\omega}{2\pi i \omega} \sum_{j=1}^{\infty} \left[\prod_{i=1}^j \int d^2\mathbf{q}_i \right] \frac{\Phi_A(\mathbf{q}_1)}{2\pi\mathbf{q}_1^2} \\ &\times \left[\prod_{i=1}^{j-1} \left(\frac{\mathbf{q}_{i+1}^2}{\mathbf{q}_i^2} \right)^{\frac{\omega}{2}} \frac{1}{\omega} \mathcal{K}(\mathbf{q}_i, \mathbf{q}_{i+1}) \right] \left(\frac{\mathbf{k}_J^2}{\mathbf{q}_a^2} \right)^{\frac{\omega}{2}} \mathcal{V}(\mathbf{q}_a, \mathbf{q}_b; \mathbf{k}_J, y_J) \left(\frac{s_{AJ}}{\mathbf{k}_J^2} \right)^{\omega} \dots (43) \end{aligned}$$

These changes can be absorbed at NLO in the kernels and impact factors. The impact factors get one contribution, as can be seen in Fig. 3:

$$\tilde{\Phi}(\mathbf{k}_a) = \Phi(\mathbf{k}_a) - \frac{1}{2}\mathbf{k}_a^2 \int d^2\mathbf{q} \frac{\Phi^{(B)}(\mathbf{q})}{\mathbf{q}^2} \mathcal{K}^{(B)}(\mathbf{q}, \mathbf{k}_a) \ln \frac{\mathbf{q}^2}{\mathbf{k}_a^2}. \quad (44)$$

The kernels in the evolution receive a double contribution from the different energy scale choices of both the incoming and outgoing Reggeons (see Fig. 3). This amounts to the following correction:

$$\tilde{\mathcal{K}}(\mathbf{q}_1, \mathbf{q}_2) = \mathcal{K}(\mathbf{q}_1, \mathbf{q}_2) - \frac{1}{2} \int d^2\mathbf{q} \mathcal{K}^{(B)}(\mathbf{q}_1, \mathbf{q}) \mathcal{K}^{(B)}(\mathbf{q}, \mathbf{q}_2) \ln \frac{\mathbf{q}^2}{\mathbf{q}_2^2}. \quad (45)$$

There is a different type of term in the case of the emission vertex where the jet is defined. This correction has also two contributions originated at the two different evolution chains from the hadrons A and B :

$$\begin{aligned} \tilde{\mathcal{V}}(\mathbf{q}_a, \mathbf{q}_b) &= \mathcal{V}(\mathbf{q}_a, \mathbf{q}_b) - \frac{1}{2} \int d^2\mathbf{q} \mathcal{K}^{(B)}(\mathbf{q}_a, \mathbf{q}) \mathcal{V}^{(B)}(\mathbf{q}, \mathbf{q}_b) \ln \frac{\mathbf{q}^2}{(\mathbf{q} - \mathbf{q}_b)^2} \\ &\quad - \frac{1}{2} \int d^2\mathbf{q} \mathcal{V}^{(B)}(\mathbf{q}_a, \mathbf{q}) \mathcal{K}^{(B)}(\mathbf{q}, \mathbf{q}_b) \ln \frac{\mathbf{q}^2}{(\mathbf{q}_a - \mathbf{q})^2}. \quad (46) \end{aligned}$$

The final expression for the cross section in the asymmetric case is

$$\begin{aligned} \frac{d\sigma}{d^2\mathbf{k}_J dy_J} &= \int d^2\mathbf{q}_a \int d^2\mathbf{k}_a \frac{\tilde{\Phi}_A(\mathbf{k}_a)}{2\pi\mathbf{k}_a^2} \\ &\quad \times \int \frac{d\omega}{2\pi i} \tilde{f}_\omega(\mathbf{k}_a, \mathbf{q}_a) \left(\frac{s_{AJ}}{\mathbf{k}_J^2} \right)^{\omega} \tilde{\mathcal{V}}(\mathbf{q}_a, \mathbf{q}_b; \mathbf{k}_J, y_J) \dots (47) \end{aligned}$$

It is interesting to discuss the NLO unintegrated gluon density in this context. It is defined by

$$g(x, \mathbf{k}) = \int d^2\mathbf{q} \frac{\tilde{\Phi}_P(\mathbf{q})}{2\pi\mathbf{q}^2} \int \frac{d\omega}{2\pi i} \tilde{f}_\omega(\mathbf{k}, \mathbf{q}) x^{-\omega}, \quad (48)$$

where the gluon Green's function \tilde{f}_ω is the solution to a new BFKL equation with the modified kernel which includes the energy shift at NLO:

$$\omega \tilde{f}_\omega(\mathbf{k}_a, \mathbf{q}_a) = \delta^{(2)}(\mathbf{k}_a - \mathbf{q}_a) + \int d^2\mathbf{q} \tilde{\mathcal{K}}(\mathbf{k}_a, \mathbf{q}) \tilde{f}_\omega(\mathbf{q}, \mathbf{q}_a). \quad (49)$$

The unintegrated gluon distribution then follows the evolution equation

$$\frac{\partial g(x, \mathbf{q}_a)}{\partial \ln 1/x} = \int d^2\mathbf{q} \tilde{\mathcal{K}}(\mathbf{q}_a, \mathbf{q}) g(x, \mathbf{q}). \quad (50)$$

Finally, taking into account the evolution from the other hadron, the differential cross section reads

$$\frac{d\sigma}{d^2\mathbf{k}_J dy_J} = \int d^2\mathbf{q}_a \int d^2\mathbf{q}_b g(x_a, \mathbf{q}_a) g(x_b, \mathbf{q}_b) \tilde{\mathcal{V}}(\mathbf{q}_a, \mathbf{q}_b; \mathbf{k}_J, y_J). \quad (51)$$

It is worth mentioning that the proton impact factor contains non-perturbative physics which can only be modeled by, *e.g.*

$$\Phi_P(\mathbf{q}) \sim (1-x)^{p_1} x^{-p_2} \left(\frac{\mathbf{q}^2}{\mathbf{q}^2 + Q_0^2} \right)^{p_3}, \quad (52)$$

where p_i are positive free parameters and Q_0^2 representing a momentum scale of the order of the confinement scale.

5. Azimuthal angle decorrelations in Mueller–Navelet jets at hadron colliders

In [30] azimuthal angle decorrelations in inclusive dijet cross sections were studied analytically including the BFKL kernel in the NLLA while keeping the jet vertices at leading order. The angular decorrelation for jets with a wide separation in rapidity decreases when NLO effects are included.

BFKL effects should dominate in observables with a large center-of-mass energy, and two large and similar transverse scales. This is the case of the inclusive hadroproduction of two jets with large and similar transverse momenta and a large relative separation in rapidity, Y . These are the so-called Mueller–Navelet jets, first proposed in Ref. [31]. A rise with Y in the partonic cross section was predicted in agreement with the LLA hard Pomeron intercept. At hadronic level Mueller–Navelet jets are produced in a region of fast falling of the parton distributions, reducing this rise. BFKL enhances soft real emission as Y increases reducing the angular correlation. This was investigated in the LLA in Ref. [32, 33, 34]. The decorrelation lies quite below the experimental data [35, 36, 37, 38] at the Tevatron.

We now investigate the cross section parton + parton \rightarrow jet + jet + soft emission, with the two jets having transverse momenta \vec{q}_1 and \vec{q}_2 and with a relative rapidity separation Y . The differential partonic cross section is

$$\frac{d\hat{\sigma}}{d^2\vec{q}_1 d^2\vec{q}_2} = \frac{\pi^2 \bar{\alpha}_s^2}{2} \frac{f(\vec{q}_1, \vec{q}_2, Y)}{q_1^2 q_2^2}, \quad (53)$$

We work with the Mellin transform:

$$f(\vec{q}_1, \vec{q}_2, Y) = \int \frac{d\omega}{2\pi i} e^{\omega Y} f_\omega(\vec{q}_1, \vec{q}_2). \quad (54)$$

The solution to the BFKL equation in the LLA is

$$f_\omega(\vec{q}_1, \vec{q}_2) = \frac{1}{2\pi^2} \sum_{n=-\infty}^{\infty} \int_{-\infty}^{\infty} d\nu (q_1^2)^{-i\nu - \frac{1}{2}} (q_2^2)^{i\nu - \frac{1}{2}} \frac{e^{in(\theta_1 - \theta_2)}}{\omega - \bar{\alpha}_s \chi_0(|n|, \nu)} \quad (55)$$

with

$$\chi_0(n, \nu) = 2\psi(1) - \psi\left(\frac{1}{2} + i\nu + \frac{n}{2}\right) - \psi\left(\frac{1}{2} - i\nu + \frac{n}{2}\right), \quad (56)$$

The BFKL equation for non-zero momentum transfer is of Schrödinger-like type with a holomorphically separable Hamiltonian. Both the holomorphic and antiholomorphic sectors are invariant under spin zero Möbius transformations with eigenfunctions carrying a conformal weight of the form $\gamma = \frac{1}{2} + i\nu + \frac{n}{2}$. In the principal series of the unitary representation ν is real and $|n|$ the integer conformal spin [39]. Hence, extracting information about n is equivalent to proving the conformal structure of high energy QCD.

We now integrate over the phase space of the two emitted gluons together with some general jet vertices, *i.e.*

$$\hat{\sigma}(\alpha_s, Y, p_{1,2}^2) = \int d^2\vec{q}_1 \int d^2\vec{q}_2 \Phi_{\text{jet}_1}(\vec{q}_1, p_1^2) \Phi_{\text{jet}_2}(\vec{q}_2, p_2^2) \frac{d\hat{\sigma}}{d^2\vec{q}_1 d^2\vec{q}_2}. \quad (57)$$

In the jet vertices only leading-order terms are kept:

$$\Phi_{\text{jet}_i}^{(0)}(\vec{q}, p_i^2) = \theta(q^2 - p_i^2), \quad (58)$$

where p_i^2 corresponds to a resolution scale for the gluon jet. To extend this analysis it is needed to use the NLO jet vertices in Ref. [40, 41] where the definition of a jet is much more complex than here. We can now write

$$\hat{\sigma} = \frac{\pi^2 \bar{\alpha}_s^2}{2} \int d^2\vec{q}_1 \int d^2\vec{q}_2 \frac{\Phi_{\text{jet}_1}^{(0)}(\vec{q}_1, p_1^2)}{q_1^2} \frac{\Phi_{\text{jet}_2}^{(0)}(\vec{q}_2, p_2^2)}{q_2^2} f(\vec{q}_1, \vec{q}_2, Y). \quad (59)$$

In a transverse momenta operator representation:

$$\langle \vec{q} | \nu, n \rangle = \frac{1}{\pi\sqrt{2}} (q^2)^{i\nu-\frac{1}{2}} e^{in\theta}, \quad (60)$$

the action of the NLO kernel, calculated in Ref. [42], is

$$\begin{aligned} \hat{K} | \nu, n \rangle = & \left\{ \bar{\alpha}_s \chi_0(|n|, \nu) + \bar{\alpha}_s^2 \chi_1(|n|, \nu) \right. \\ & \left. + \bar{\alpha}_s^2 \frac{\beta_0}{8N_c} \left[2 \chi_0(|n|, \nu) \left(i \frac{\partial}{\partial \nu} + \log \mu^2 \right) + \left(i \frac{\partial}{\partial \nu} \chi_0(|n|, \nu) \right) \right] \right\} | \nu, n \rangle, \end{aligned} \quad (61)$$

where χ_1 , for a general conformal spin, reads

$$\begin{aligned} \chi_1(n, \gamma) = & \mathcal{S} \chi_0(n, \gamma) + \frac{3}{2} \zeta(3) - \frac{\beta_0}{8N_c} \chi_0^2(n, \gamma) \\ & + \frac{1}{4} \left[\psi'' \left(\gamma + \frac{n}{2} \right) + \psi'' \left(1 - \gamma + \frac{n}{2} \right) - 2 \phi(n, \gamma) - 2 \phi(n, 1 - \gamma) \right] \\ & - \frac{\pi^2 \cos(\pi\gamma)}{4 \sin^2(\pi\gamma) (1 - 2\gamma)} \left\{ \left[3 + \left(1 + \frac{n_f}{N_c^3} \right) \frac{2 + 3\gamma(1 - \gamma)}{(3 - 2\gamma)(1 + 2\gamma)} \right] \delta_{n0} \right. \\ & \left. - \left(1 + \frac{n_f}{N_c^3} \right) \frac{\gamma(1 - \gamma)}{2(3 - 2\gamma)(1 + 2\gamma)} \delta_{n2} \right\}, \end{aligned} \quad (62)$$

with $\mathcal{S} = (4 - \pi^2 + 5\beta_0/N_c)/12$, $\beta_0 = (11N_c - 2n_f)/3$. ϕ can be found in [42].

The jet vertices on the basis in Eq. (60) are:

$$\int d^2 \vec{q} \frac{\Phi_{\text{jet}_1}^{(0)}(\vec{q}, p_1^2)}{q^2} \langle \vec{q} | \nu, n \rangle = \frac{1}{\sqrt{2}} \frac{1}{\left(\frac{1}{2} - i\nu\right)} (p_1^2)^{i\nu-\frac{1}{2}} \delta_{n,0} \equiv c_1(\nu) \delta_{n,0}, \quad (63)$$

with the $c_2(\nu)$ projection of $\Phi_{\text{jet}_2}^{(0)}$ on $\langle n, \nu | \vec{q} \rangle$ being the complex conjugate of (63) with p_1^2 being replaced by p_2^2 . The cross section now reads

$$\begin{aligned} \hat{\sigma} = & \frac{\pi^2 \bar{\alpha}_s^2}{2} \sum_{n=-\infty}^{\infty} \int_{-\infty}^{\infty} d\nu e^{\bar{\alpha}_s \chi_0(|n|, \nu) Y} c_1(\nu) c_2(\nu) \delta_{n,0} \left\{ 1 + \bar{\alpha}_s^2 Y \right. \\ & \left. \times \left[\chi_1(|n|, \nu) + \frac{\beta_0}{4N_c} \left(\log(\mu^2) + \frac{i}{2} \frac{\partial}{\partial \nu} \log \left(\frac{c_1(\nu)}{c_2(\nu)} \right) + \frac{i}{2} \frac{\partial}{\partial \nu} \right) \chi_0(|n|, \nu) \right] \right\}. \end{aligned} \quad (64)$$

For the LO jet vertices the logarithmic derivative in Eq. (65) is

$$-i \frac{\partial}{\partial \nu} \log \left(\frac{c_1(\nu)}{c_2(\nu)} \right) = \log(p_1^2 p_2^2) + \frac{1}{\frac{1}{4} + \nu^2}. \quad (65)$$

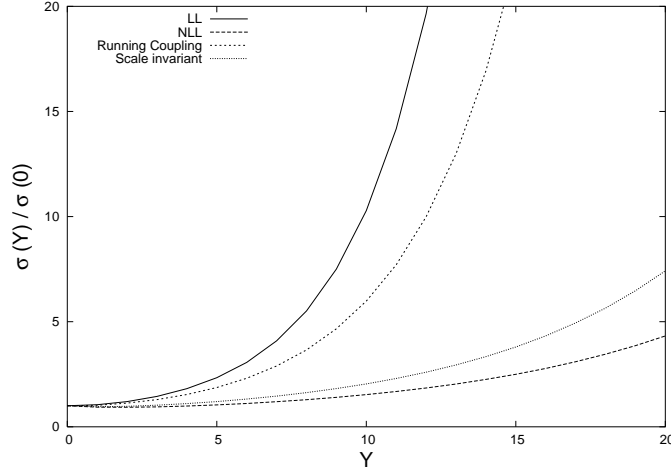


Fig. 4. Partonic cross section growth with the rapidity separation of the dijets.

If $\phi = \theta_1 - \theta_2 - \pi$, in the case of two equal resolution momenta, $p_1^2 = p_2^2 \equiv p^2$, the angular differential cross section can be expressed as

$$\frac{d\hat{\sigma}(\alpha_s, Y, p^2)}{d\phi} = \frac{\pi^3 \bar{\alpha}_s^2}{2p^2} \frac{1}{2\pi} \sum_{n=-\infty}^{\infty} e^{in\phi} \mathcal{C}_n(Y), \quad (66)$$

with

$$\mathcal{C}_n(Y) = \int_{-\infty}^{\infty} \frac{d\nu}{2\pi} e^{\bar{\alpha}_s(p^2)Y \left(\chi_0(|n|, \nu) + \bar{\alpha}_s(p^2) \left(\chi_1(|n|, \nu) - \frac{\beta_0}{8N_c} \frac{\chi_0(|n|, \nu)}{\left(\frac{1}{4} + \nu^2\right)} \right) \right)} \frac{1}{\left(\frac{1}{4} + \nu^2\right)}. \quad (67)$$

$n = 0$ governs the energy dependence of the cross section:

$$\hat{\sigma}(\alpha_s, Y, p^2) = \frac{\pi^3 \bar{\alpha}_s^2}{2p^2} \mathcal{C}_0(Y). \quad (68)$$

In the plots we take $p = 30$ GeV, $n_f = 4$ and $\Lambda_{\text{QCD}} = 0.1416$ GeV. The $n = 0$ coefficient is directly related to the normalized cross section

$$\frac{\hat{\sigma}(Y)}{\hat{\sigma}(0)} = \frac{\mathcal{C}_0(Y)}{\mathcal{C}_0(0)}. \quad (69)$$

The rise with Y of this observable is shown in Fig. 4. Clearly the NLL intercept is very much reduced with respect to the LL case. The remaining

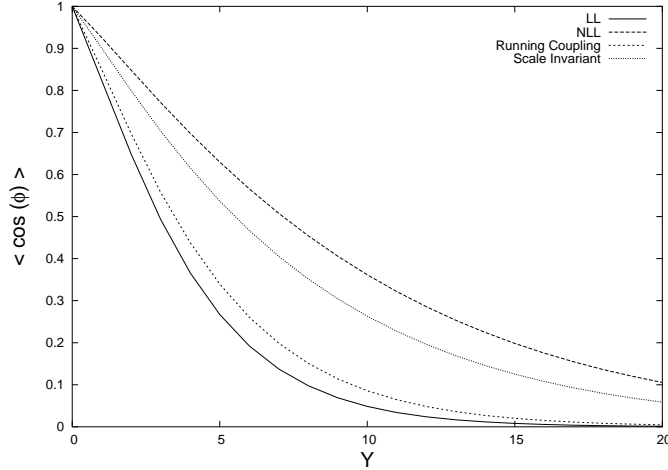


Fig. 5. Dijet azimuthal angle correlation as a function of the rapidity separation.

coefficients with $n \geq 1$ all decrease with Y . Because of this the angular correlations also diminish as the rapidity interval between the jets gets larger. This point can be studied in detail using the mean values

$$\langle \cos(m\phi) \rangle = \frac{\mathcal{C}_m(Y)}{\mathcal{C}_0(Y)}. \quad (70)$$

$\langle \cos(\phi) \rangle$ is calculated in Fig. 5. The NLL effects decrease the azimuthal angle decorrelation. This is the case for the running of the coupling and also for the scale invariant terms. This is encouraging from the phenomenological point of view given that the data at the Tevatron typically have lower decorrelation than predicted by LLA BFKL or LLA with running coupling. The difference in the decorrelation between LLA and NLLA is driven by the $n = 0$ conformal spin since the ratio

$$\frac{\langle \cos(\phi) \rangle^{\text{NLLA}}}{\langle \cos(\phi) \rangle^{\text{LLA}}} = \frac{\mathcal{C}_1^{\text{NLLA}}(Y) \mathcal{C}_0^{\text{LLA}}(Y)}{\mathcal{C}_0^{\text{NLLA}}(Y) \mathcal{C}_1^{\text{LLA}}(Y)}, \quad (71)$$

is always close to one

$$1.2 > \frac{\mathcal{C}_1^{\text{NLLA}}(Y)}{\mathcal{C}_1^{\text{LLA}}(Y)} > 1. \quad (72)$$

This is a consequence of the good convergence in terms of asymptotic intercepts of the NLLA BFKL calculation for conformal spins larger than zero. For completeness the $m = 2, 3$ cases for $\langle \cos(m\phi) \rangle$ are shown in Fig. 6.

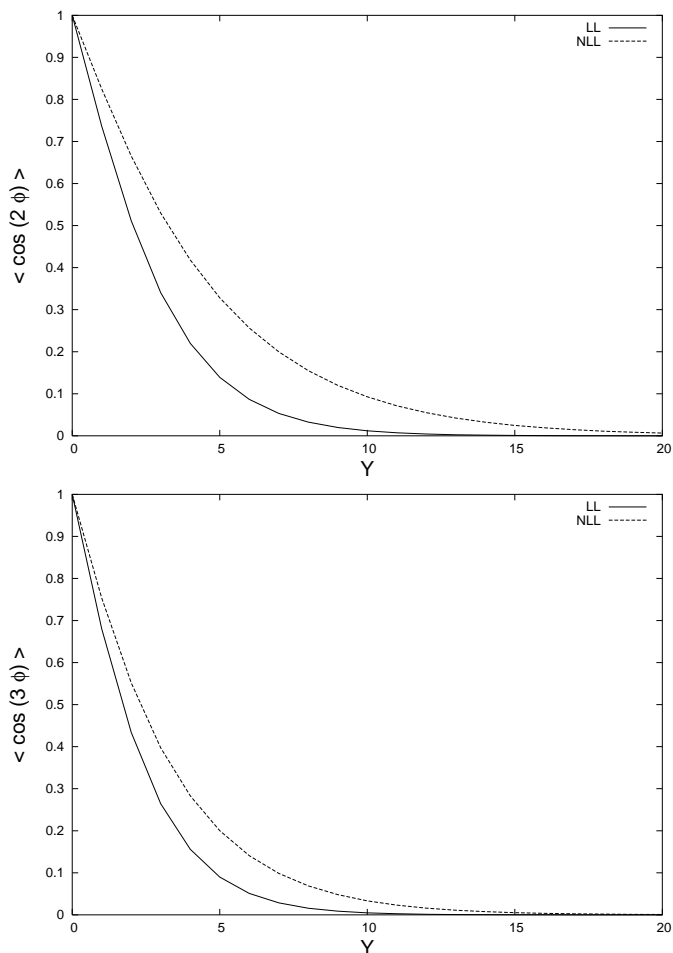


Fig. 6. Dijet azimuthal angle decorrelation as a function of their separation in rapidity.

These distributions test the structure of the higher conformal spins. The methods of this section have been applied to phenomenology of dijets at the Tevatron and the LHC in [43, 44], and to the production of forward jets in DIS at HERA in [45].

REFERENCES

- [1] L. N. Lipatov, Sov. J. Nucl. Phys. **23** (1976) 338.
- [2] V. S. Fadin, E. A. Kuraev, L. N. Lipatov, Phys. Lett. B **60** (1975) 50.

- [3] E. A. Kuraev, L. N. Lipatov, V. S. Fadin, Sov. Phys. JETP **44** (1976) 443.
- [4] E. A. Kuraev, L. N. Lipatov, V. S. Fadin, Sov. Phys. JETP **45** (1977) 199.
- [5] I. I. Balitsky, L. N. Lipatov, Sov. J. Nucl. Phys. **28** (1978) 822.
- [6] S. Catani, F. Fiorani and G. Marchesini, Phys. Lett. **B234**, 339 (1990).
- [7] G. Marchesini, Nucl. Phys. **B445**, 49 (1995).
- [8] M. Ciafaloni, Nucl. Phys. **B296**, 49 (1988).
- [9] S. Catani, F. Fiorani, G. Marchesini and G. Oriani, Nucl. Phys. **B361**, 645 (1991).
- [10] J. R. Forshaw and A. Sabio Vera, Phys. Lett. **B440** (1998) 141.
- [11] J. R. Forshaw, A. Sabio Vera and B. R. Webber, J. Phys. G **G25** (1999) 1511.
- [12] B. R. Webber, Phys. Lett. **B444** (1998) 81.
- [13] C. Ewerz and B. R. Webber, JHEP **9904** (1999) 022.
- [14] C. Ewerz and B. R. Webber, JHEP **9908** (1999) 019.
- [15] G. P. Salam, JHEP **9903** (1999) 009.
- [16] M. Dittmar *et al.*, arXiv:hep-ph/0511119.
- [17] S. Alekhin *et al.*, arXiv:hep-ph/0601012.
- [18] S. Alekhin *et al.*, arXiv:hep-ph/0601013.
- [19] J. R. Andersen *et al.* [Small x Collaboration], Eur. Phys. J. C **48** (2006) 53.
- [20] J. R. Andersen and A. Sabio Vera, Phys. Lett. B **567** (2003) 116.
- [21] J. R. Andersen and A. Sabio Vera, Nucl. Phys. B **679** (2004) 345.
- [22] J. R. Andersen and A. Sabio Vera, Nucl. Phys. B **699** (2004) 90.
- [23] J. R. Andersen and A. Sabio Vera, JHEP **0501** (2005) 045.
- [24] G. P. Salam, JHEP **9807**, 019 (1998).
- [25] A. Sabio Vera, Nucl. Phys. B **722** (2005) 65.
- [26] V. S. Fadin and L. N. Lipatov, Phys. Lett. B **429** (1998) 127.
- [27] M. Ciafaloni and G. Camici, Phys. Lett. B **430** (1998) 349.
- [28] F. Caporale, A. Papa and A. Sabio Vera, Eur. Phys. J. C **53** (2008) 525.
- [29] J. Bartels, A. Sabio Vera and F. Schwennsen, JHEP **0611** (2006) 051.
- [30] A. Sabio Vera, Nucl. Phys. B **746** (2006) 1.
- [31] A. H. Mueller and H. Navelet, Nucl. Phys. B **282** (1987) 727.
- [32] V. Del Duca and C. R. Schmidt, Phys. Rev. D **49** (1994) 4510.
- [33] V. Del Duca and C. R. Schmidt, Phys. Rev. D **51** (1995) 2150.
- [34] W. J. Stirling, Nucl. Phys. B **423** (1994) 56.
- [35] S. Abachi *et al.* [D0 Collaboration], Phys. Rev. Lett. **77**, 595 (1996).
- [36] B. Abbott *et al.* [D0 Collaboration], Phys. Rev. Lett. **84**, 5722 (2000).
- [37] B. Abbott *et al.* [D0 Collaboration], Phys. Rev. Lett. **80**, 666 (1998).
- [38] F. Abe *et al.* [CDF Collaboration], Phys. Rev. Lett. **77**, 5336 (1996) [Erratum-*ibid.* **78**, 4307 (1997)].

- [39] L. N. Lipatov, Sov. Phys. JETP **63**, 904 (1986) [Zh. Eksp. Teor. Fiz. **90**, 1536 (1986)].
- [40] J. Bartels, D. Colferai and G. P. Vacca, Eur. Phys. J. C **24**, 83 (2002).
- [41] J. Bartels, D. Colferai and G. P. Vacca, Eur. Phys. J. C **29**, 235 (2003).
- [42] A. V. Kotikov and L. N. Lipatov, Nucl. Phys. B **582**, 19 (2000).
- [43] A. Sabio Vera and F. Schwennsen, Nucl. Phys. B **776** (2007) 170.
- [44] C. Marquet and C. Royon, arXiv:0704.3409 [hep-ph].
- [45] A. Sabio Vera and F. Schwennsen, Phys. Rev. D **77** (2008) 014001.